



Experiment title: High-resolution small-angle microdiffraction studies of order/disorder in colloidal crystals

**Experiment number:
26-02-101**

Beamline:
BM-26

Date(s) of experiment:
From: 9-03-2002
To: 13-03-2002

Date of report:
30-09-2002

Shifts:
12

Local contact(s):
Igor Dolbnya

Names and affiliations of applicants (* indicates experimentalists):

Igor Dolbnya*, DUBBLE, ESRF; Andrei Petukhov*, Dirk Aarts*, Xinyi Xian*, Gert Jan Vroege, Henk Lekkerkerker, van 't Hoff laboratory for physical and colloid chemistry, Utrecht

Report: (max. 2 pages)

This experiment was devoted to optimisation of the DUBBLE BM-26 beam line to obtain best resolution for small-angle x-ray diffraction on colloidal crystals. The samples are described elsewhere [1,2].

The main factors limiting our resolution are the beam coherence and the detector resolution. The quality of the x-ray beam can be expressed in terms of its longitudinal and transverse coherence length. Our estimates [1] showed that the spectral width (at DUBBLE $\Delta\lambda/\lambda = 2 \times 10^{-4}$) does not limit our resolution in the longitudinal direction under the conditions of our small-angle diffraction experiment. The main attention was therefore paid to detectors and the transverse coherence. As detectors we have used a CCD camera (with the resolution of $\sim 55 \mu\text{m}$ instead of $\sim 255 \mu\text{m}$ of the conventional gas-filled multi-wire 2D detector) and high-resolution ($1-2 \mu\text{m}$) x-ray films. The transverse coherence length is limited by the angular size of the source seen from the position of the sample. In addition, it may be reduced by imperfectness of optical elements and X-ray windows in a beamline path. Significant efforts were spent for careful alignment of the whole optical and instrumental set-up. The slit sizes were also optimised. Figure 1 demonstrates that we were able to create conditions for (nearly) coherent irradiation of the sample. While the direct beam (Fig. 1a) possesses a smooth variation of intensity, the diffracted peaks display a well-developed speckle structure, which we have assigned to imperfectness of the Bragg-reflecting planes.

Figure 2 illustrates the obtained resolution on a CCD camera, which is improved by nearly one order of magnitude (compared with patterns in our previous reports).

The diffraction pattern in panel (a) is taken with an exposure time of 0.1 s and none of the diffraction peaks saturate the CCD camera. However, since the dynamic range (the ratio of the maximum detectable signal to the noise level) of the camera is only about 1000, the weaker features of the diffraction pattern are not visible. The latter can be seen in panels (b) and (c), which present the same diffraction pattern taken with longer exposure. The brightest reflections strongly over-saturate the CCD camera, especially in panel (c) leading, in particular, to artificial vertical stripes.

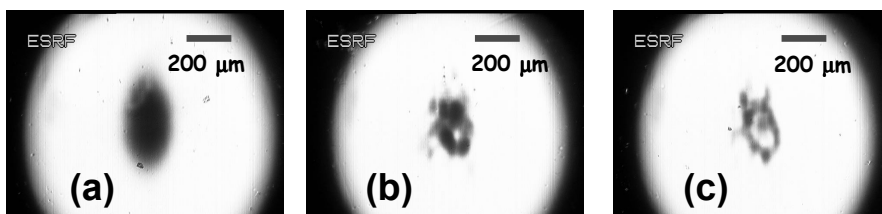


Figure 1. High-resolution x-ray film images of the direct beam (a) and two low-order crystal reflections (b) and (c). Speckle structure in (b) and (c) reflects imperfectness of Bragg-reflecting crystal planes.

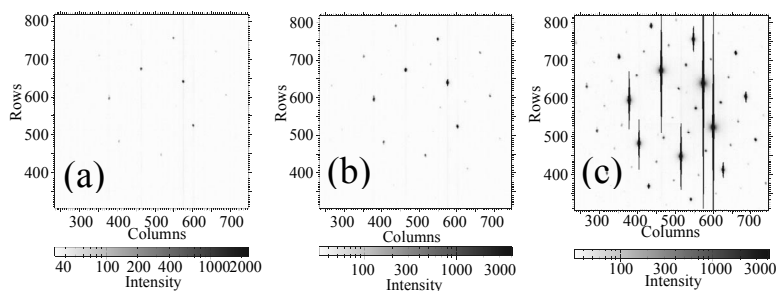


Figure 2. Zoom into the central part of the diffraction patterns obtained with the x-ray beam normal to the hexagonal planes and an exposure time $t = 0.1$ s (a), 1 s (b) and 60 s (c).

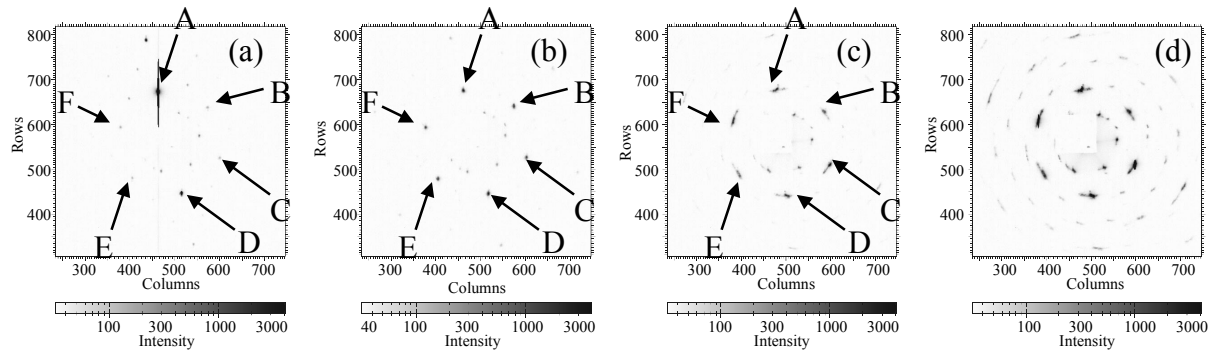


Figure 3. Modification of the diffraction pattern during sample drying. (a) Meniscus is well above the sediment; (b) meniscus is (nearly) flat; (c) meniscus turns upside-down, air comes into sediment along the sides of the capillary; (d) crystal dries. Exposure time is 10 s (a, d) and 15 s (b, c).

We have recorded the modification of the single crystal diffraction patterns during drying. This study is of importance since dried crystals possessing higher contrast are more suitable for photonic applications. Simultaneously, visual control of the sample was performed with the TV camera installed in the experimental hutch. The diffraction patterns were recorded as a function of time within a fixed area of the sample and at a fixed orientation. We have tilted the crystal by $\sim 0.4^\circ$ relative to the orientation used in Fig. 2. In this case we can achieve reciprocal space resolution $\sim 10^{-6}$ of the x-ray wavevector [1] by observing the decay of diffraction peaks. Two reflections (marked A and D) in Fig. 3a are very close to the Ewald sphere and strongly over-saturate the CCD detector. The other four (110)-class spots (B, C, E, F) are much weaker because of the tilt-induced mismatch of the very sharp crystal reflections. However, when the meniscus touches the sediment, the capillary forces induce a strain field, which presumably bends the crystal leading to broadening of the reflections. This can be seen in panel (b): while the brightest two reflections A and D decay, the other four come up. Then, in panel (c) the crystal is seen to be not able anymore to withstand the too strong strain field induced by the capillary forces: it breaks into smaller crystallites. Note, that the crystal is still wet. Finally, it dries as can be seen in panel (d): the contrast of the pattern increases. No significant change in the shape of the reflections is seen in (d).

Figure 4 presents another example of our results where the improved on-detector resolution was crucial. Earlier, our sedimentary crystals seemed to have random-stacking hexagonal close-packed (rhcp) structure with the stacking probability α of finding an fcc stacking sequence close to $\alpha = 0.5$ [1,2]. Due to the stacking-disorder-induced lack of periodicity, the reciprocal lattice of rhcp crystals possesses Bragg scattering rods [2]. The latter were directly visualised on the detector in our previous experiment [2]. Figure 3a presents a similar diffraction pattern, showing a set of bright stacking-independent spots and a Bragg scattering rod. The intensity distribution along the rod (broad maxima at half-integer values of l) closely corresponds to $\alpha = 0.5$ [1,2]. However, additional sharp reflections are now resolved along the Bragg rod. They appear at $l = n - 1/3$, where n is any integer. These sharp reflections can be explained by the presence of a single-domain fcc crystal with one of its (111) planes attached to the hexagonal planes of the rhcp single crystal. Note that the volume of the fcc crystal (which could be estimated by integrating the intensity within one reflection) is small compared to the volume of the rhcp crystal (proportional to the integral along the rod within one period of the structure factor). This finding might have an impact on our understanding of hard-sphere crystallisation. The common belief is that the metastable rhcp crystals may have various values of the stacking parameter α . Our result, instead, suggests that α has a discrete spectrum and can only take one of the values of 0.5 (in rhcp) and 1 (in fcc).

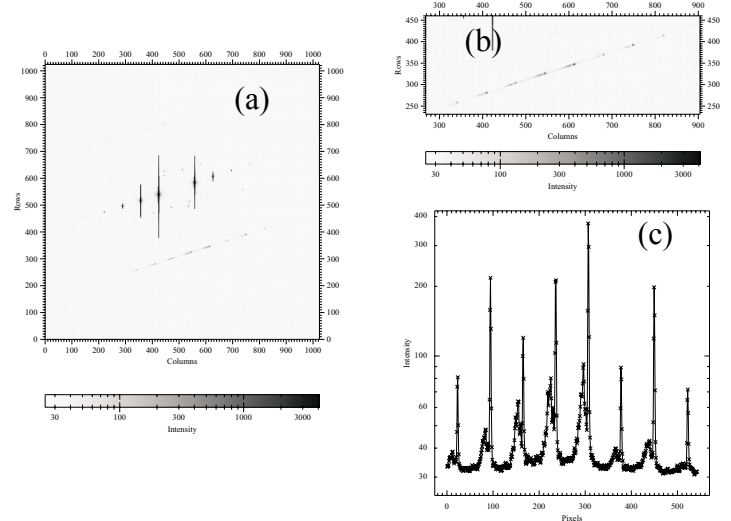


Figure 4. Coexistence of rhcp and fcc crystals: (a) full diffraction pattern and (b) a zoom into the scattering rod region. (c) A slice of the diffracted intensity along the rod.

References

- [1] A.V. Petukhov et al., Phys. Rev. Lett., **88**, 208301 (2002).
- [2] report, experiment 26-02-90 (September 2001).